J Mater Sci (2006) 41:8372–8376
DOI 10.1007/s10853-006-0910-1

LETTER

Tensile ductility at room temperature of nanocrystalline Ni–W alloy

Hiroyuki Hosokawa · Hiroshi Matsumoto · Masataka Hakamada · Mamoru Mabuchi

Received: 5 June 2006 / Accepted: 1 September 2006 / Published online: 11 November 2006

The nature of deformation in a polycrystalline metal changes with grain size. In a coarse-grained metal with a grain size larger than 1000–100 nm, plastic deformation occurs due to intragranular dislocations which are continuously nucleated from Frank-Read sources. When the grain size is smaller than 1000–100 nm, nucleation of dislocations from Frank-Read sources is suppressed because the stress required for their operation is inversely proportional to the size of sources. Molecular dynamics (MD) simulations [1–4] and experiments [5, 6] revealed that partial or perfect dislocations are emitted from grain boundaries, and deformation twinning and stacking faults are formed in ultrafine-grained and nanocrystalline metals with a grain size of 1000–10 nm. Such ultrafine-grained and nanocrystalline metals often exhibit an extraordinary combination of high strength and high ductility [7]. In coarse-grained and ultrafine-grained metals, an intragranular dislocation-based deformation process is dominant and the strength increases with decreasing grain size (the ''Hall–Petch effect''). However, MD simulation [8–10] suggests that below a critical grain size, which is approximately 10 nm, the dominant deformation process is an intragranular grain-boundary-based process such as grain boundary sliding, and the strength decreases with decreasing grain size (the ''inverse Hall–Petch effect''). Some experimental results [11–13] also verified existence of the inverse Hall–Petch effect. However, most of the experiments on nanocrystalline metals with a grain size below the critical size were conducted by hardness testing.

In this letter, we show the tensile properties of nanocrystalline Ni with a grain size of approximately 6 nm. In metals with a grain size above the critical size, tensile ductility is controlled by plastic instability involving strain hardening [14]. However, the present letter shows that in a nanocrystalline metal with a grain size below the critical size, tensile ductility is not affected by plastic instability, but is strongly affected by an accommodation process for thermally activated glide of grain-boundary line defects.

To elucidate the nature of plastic deformation in the intragranular grain-boundary-based process region, the ability to distinguish a nanocrystalline metal whose grain size is below the critical size from a nanocrystalline metal whose grain size is above the critical size is required, because their respective deformation mechanisms are intrinsically different. The mechanical properties of nanocrystalline metals whose grain size is above the critical size have been investigated experimentally by tensile testing [15, 16], and it was demonstrated that high strength and high ductility are often obtained [7]. For a nanocrystalline metal whose grain size is below the critical size, however, there have been a very limited number of experimental results obtained by tensile testing [17, 18]. Experimental investigation by tensile testing on a nanocrystalline

H. Hosokawa (✉)
Materials Research Institute for Sustainable Development, National Institute of Advanced Industrial Science and Technology, 2266-98 Shimo-Shidami, Moriyama-ku, Nagoya 463-8560, Japan
e-mail: h-hosokawa@aist.go.jp

H. Matsumoto · M. Hakamada · M. Mabuchi
Department of Energy Science & Technology, Graduate School of Energy Science, Kyoto University, Yoshidahonmachi, Sakyo-ku, Kyoto 606-8501, Japan

metal whose grain size is below the critical size leads to elucidation of deformation and fracture mechanisms in the intragranular grain-boundary-based process region.

It is known that ductility is often reduced by internal flaws in nanocrystalline metals [23]. In the present study, a nanocrystalline Ni–22at.%W without flaws was prepared by an electrodeposition technique with an electrolyte of $NiSO_4{\cdot}6H_2O$: 0.06 mol/l, $Na_3C_6H_5O_7{\cdot}2H_2O$: 0.25 mol/l, $Na_2WO_4{\cdot}2H_2O$: 0.14 mol/l, $(NH_4)_2SO_4$: 0.25 mol/l, at a temperature of 333 K and a current density of 0.05 A/cm^2, using a Pt mesh anode and a Cu substrate. Because an amorphous phase partially existed in the as-deposited specimen, annealing was conducted at 353 K for 24 h in vacuum to complete crystallization and Additional annealing is also carried out to it at 353 K for 24 h (total 48 h). The microstructure of both the materials was observed by high-resolution transmission electron microscopy (HRTEM). The numbers of vacancies for both the materials were measured by positron annihilation measurements. Tensile tests were carried out at room temperature and over a wide strain rate range of $3 \times 10^{-7} - 1 \times 10^{-1}$ s^{-1}, using specimens with 8 mm in gage length, 2 mm in gage breadth and 20 μm in gage thickness.

Figure 1a shows an image of the microstructure of the nanocrystalline Ni obtained by high-resolution transmission electron microscopy (HRTEM). Flaws and pores with the size of the order of a nanometer and above were not observed. The grain size determined from HRTEM observation was 6.5 nm. Additional annealing was carried out at 353 K for 24 h in vacuum to change the grain boundary structure [20]. The microstructure of the nanocrystalline Ni after additional annealing is shown in Fig. 1b. The grain size of the annealed specimen was determined to be 6.7 nm by HRTEM observation. Figure 2 shows X-ray diffraction patterns of the nanocrystalline Ni materials. For both the materials, only broad peaks are observed, and the widths of the peaks are same, which shows that the grain growth induced by additional annealing was minor. Positron annihilation measurements revealed that the number of vacancies was decreased by additional annealing. This suggests that the specimen without additional annealing retained a vacancy-rich defect structure in its grain boundary [20], compared to the specimen with additional annealing. The critical grain size below which the inverse Hall–Petch effect holds in Ni is 7–9 nm from hardness tests [12] and around 10 nm from MD simulation [19]. Thus, the nanocrystalline Ni prepared was a nanocrystalline metal whose grain size was below the critical size.

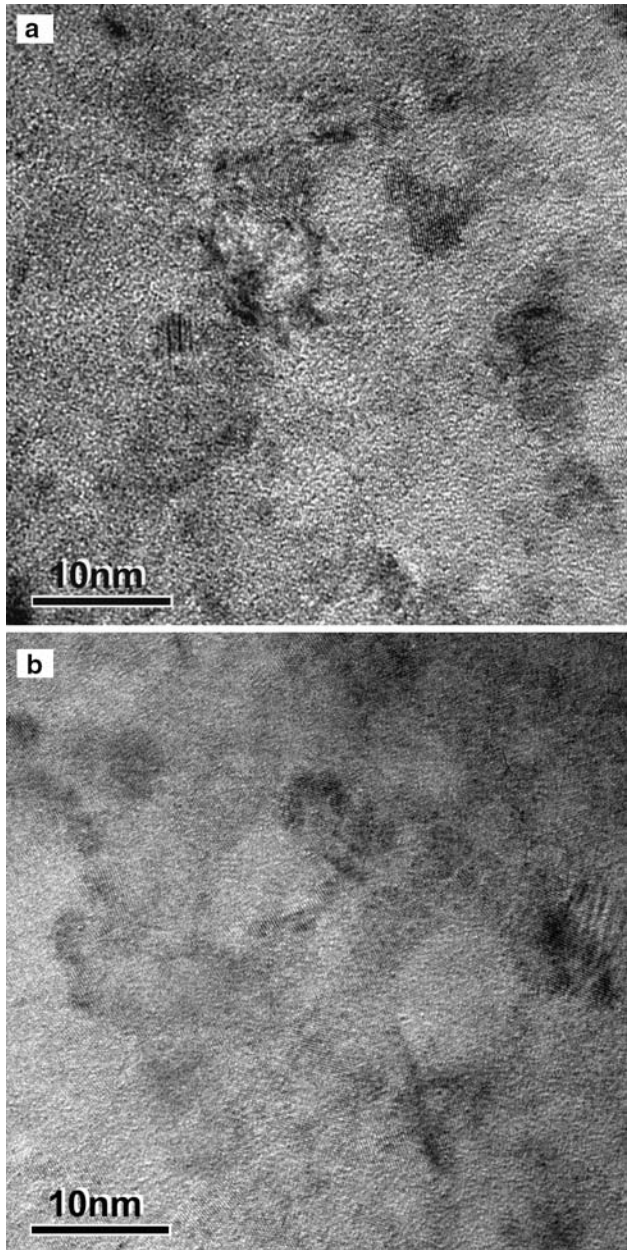

Fig. 1 HRTEM images of microstructure of nanocrystalline Ni: (**a**) a bright-field micrograph of the specimen without additional annealing and (**b**) a bright-field micrograph of the specimen with additional annealing. Additional annealing was conducted at 353 K for 24 h in vacuum

The stress–strain curves for the specimen with additional annealing (at 7×10^{-7} s^{-1}) and the specimen without additional annealing (at 3×10^{-7} s^{-1}) are shown in Fig. 3. The plastic elongation to failure was nearly 1% for the specimen without additional annealing and much less than 1% for the specimen with additional annealing. It has been reported that in ultrafine-grained or nanocrystalline metals with a grain

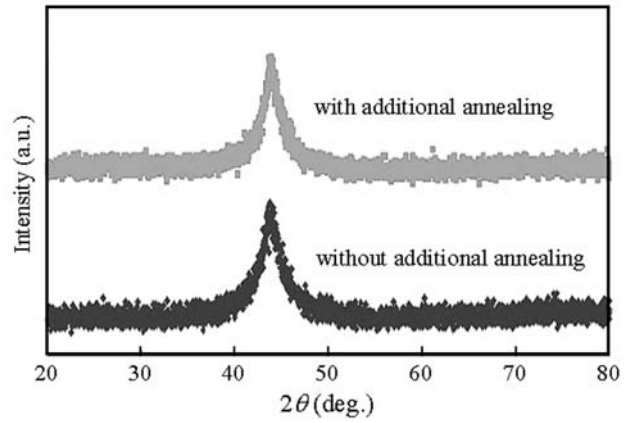

Fig. 2 X-ray diffraction patterns of nanocrystalline Ni

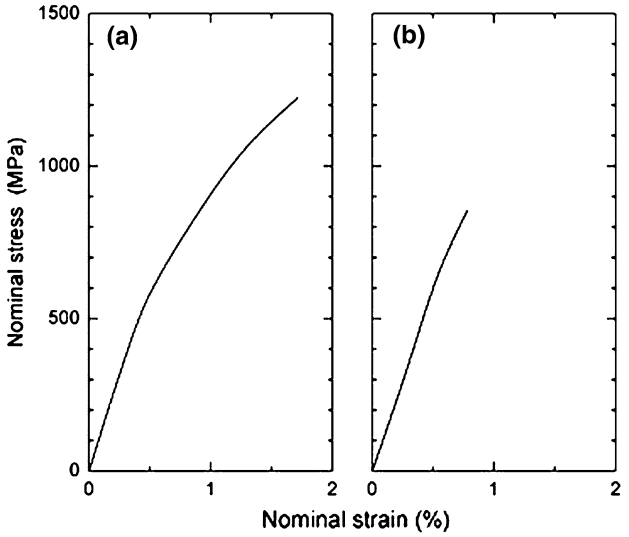

Fig. 3 The stress–strain curves for nanocrystalline Ni: (**a**) specimen without additional annealing and (**b**) specimen with additional annealing at 353 K for 24 h. The testing temperature is room temperature. The strain rate is 3×10^{-7} s^{-1} for the specimen without additional annealing and 7×10^{-7} s^{-1} for the specimen with additional annealing

size above the critical size, plastic instability strongly affects tensile ductility [14, 21]. For example, a large elongation of 65% was attained in nanocrystalline Cu due to a decrease in plastic instability caused by a strain hardening mechanism [22]. However, contrary to significant strain hardening (Fig. 3), tensile ductility was very poor in nanocrystalline Ni with a grain size below the critical size. Clearly, the mechanism that achieves high tensile ductility in a nanocrystalline metal with a grain size below the critical size is different from that in a nanocrystalline metal with a grain size above the critical size.

The variations in fracture strength, elastic limit and plastic elongation to failure as functions of strain rate for both specimens with and without additional annealing are shown in Fig. 4. The plastic elongation to failure depended on the strain rate and additional annealing (namely, the grain boundary state). Swygenhoven and Derlet [9] showed by MD simulation that two atomic processes, that is, atomic shuffling and stress-assisted diffusion can be distinguished in the interface during sliding. Moreover, MD simulation [20] revealed that the plastic strain is reduced when grain boundaries approach conditions of greater equilibrium and that similar atomic activity within the grain boundary region exists under both annealing and straining; for example, when the grain boundary structure is disordered, an increase in plastic strain occurs in the early stage of deformation, however, after a while, plastic straining is difficult. This indicates that a vacancy-rich defect structure in grain boundaries promotes the atomic processes in the interface during sliding, resulting in plastic strain; however, when vacancies are consumed in the atomic processes with straining, plastic straining is difficult. Therefore, it is suggested that the majority of plastic elongation is obtained in a transient region when moving from a nonequilibrium state to an equilibrium state in grain boundaries in a nanocrystalline metal with a grain size below the critical size. Inspection of Fig. 3 reveals that the fracture strength was hardly dependent of the strain rate and annealing. This suggests that fractures occur when vacancies are consumed and grain boundary sliding is not accommodated, irrespective of the strain rate and the amount of vacancies. This is likely to be responsible for poor ductility in a nanocrystalline metal with a grain size below the critical size.

Another important result shown in Fig. 4 is that the elastic limit depends on the strain rate. Using the theory of a thermally activated process [22], the activation volume can be given by

$$v^* = kT\frac{\delta \ln \dot{\gamma}}{\delta \tau},$$

where v^* is the activation volume, τ is the shear stress, and $\dot{\gamma}$is the shear strain rate. The activation volume was calculated to be 0.213 nm^3 for the specimen without additional annealing from the data in Fig. 4, where $\tau = \sigma/M$ ($M = 3.06$ for fcc metal). Also, from the short-range obstacle concept in the thermally activated process, the activation volume may be given by

$$v^* = bLd^*,$$

where L is the length of a defect and d^* is the size of a short-range obstacle. Assuming that L is half the grain

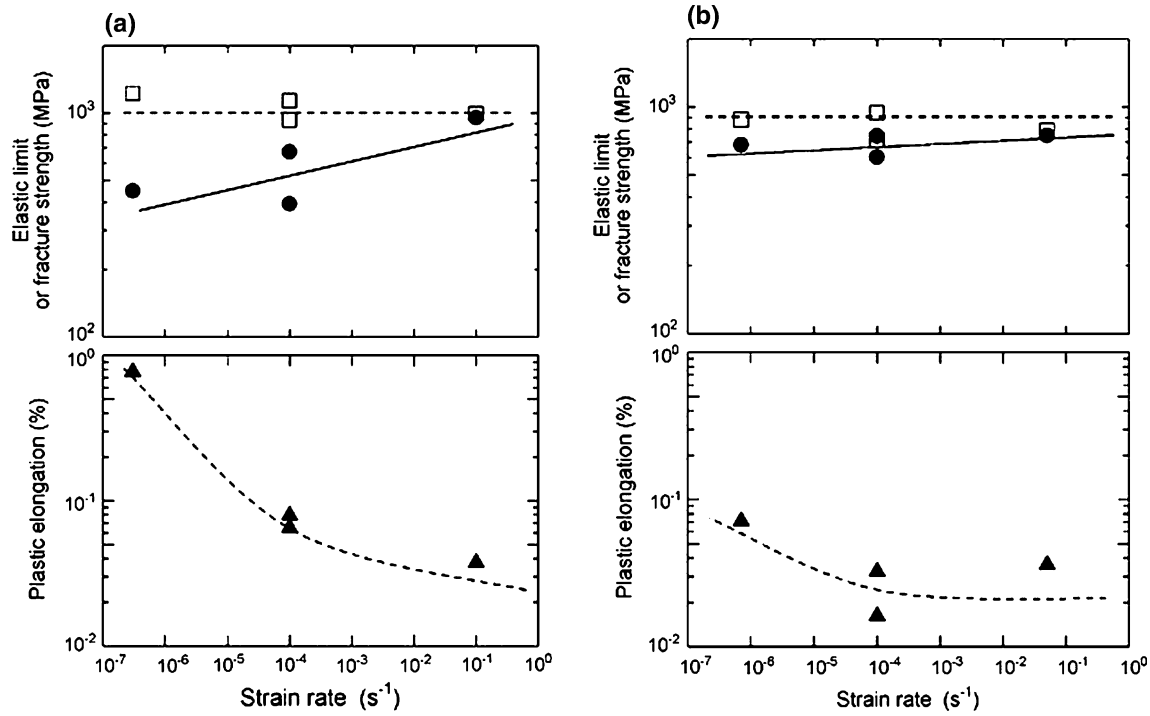

Fig. 4 The strain rate dependences of fracture strength (open square), elastic limit (solid circle) and plastic elongation (solid triangle) to failure of nanocrystalline Ni: (**a**) specimen without additional annealing and (**b**) specimen with additional annealing at 353 K for 24 h

size (=6.5/2 nm) and b is the Burgers vector of Ni (=0.25 nm), the obstacle size is calculated to be 0.26 nm, which is in agreement with or nearly equal to the atomic size of W (=0.27 nm) or the grain boundary width ($2b$) in Ni (=0.50 nm). This means that deformation at a grain boundary results from the gliding of line defects on the grain boundary; a line defect such as a dislocation plays an important role in grain-boundary-based processes and also the rate-controlling process is related to short-range obstacles such as solute atoms or high Peierls potential due to triple junctions or grain boundaries. Therefore, it is likely that vacancies are consumed for line defects to glide in the grain boundary region, resulting in strain hardening; however, after a while, vacancies are exhausted and grain boundary sliding cannot be accommodated, and finally, fracturing occurs. The fact that the specimen without additional annealing exhibited a larger plastic elongation to failure and a larger strain rate dependence of elastic limit than the specimen with additional annealing supports the hypothesis that vacancies promote accommodation for grain boundary sliding.

Acknowledgements This work was supported by ''Integrated Development of Materials and Processing Technology for High Precision Components'' by the New Energy and Industrial Technology Development Organization.

References

1. Yamakov V, Wolf D, Phillpot SR, Mukherjee AK, Gleiter H (2002) Nature Mater 1:45
2. Yamakov V, Wolf D, Phillpot SR, Gleiter H (2002) Acta Mater 50:5005
3. Bilde-Sorensen JB, Schiotz J (2003) Science 300:1244
4. Swygenhoven HV, Derlet PM, Hasnaoui A (2002) Phys Rev B 66:24101
5. Chen M, Ma E, Hemker KJ, Sheng H, Wang Y, Cheng X (2003) Science 300:1275
6. Liao XZ, Zhou F, Lavernia EJ, Srinivasan SG, Baskes MI, He DW, Zhu YT (2003) Appl Phys Lett 83:632
7. Valiev RZ, Alexandrov IV, Zhu YT, Lowe TC (2002) J. Mater Res 17:5
8. Schiotz J, Tolla FD, Jacobsen KW (1998) Nature 391:561
9. Swygenhoven HV, Derlet PM (2001) Phys Rev B 64:224105
10. Yamakov V, Wolf D, Phillpot SR, Mukherjee AK, Gleiter H (2004) Nature Mater 3:43
11. Schuh CA Nieh TG, Iwasaki H (2003) Acta Mater 51:431
12. Conrad H, Narayan J (2002) Appl Phys Lett 81:2241
13. Jia D, Wang YM, Ramesh KT, Ma E, Zhu YT, Valiev RZ (2002) Appl Phys Lett 79:611
14. Torre FD, Van Swygenhoven H, Victoria M (2002) Acta Mater 50:3957
15. Schwaiger R, Moser B, Dao M, Chollacoop N, Suresh S (2003) Acta Mater 51:5159

16. Yamasaki T (2001) Scripta Mater 44:1497
17. Iwasaki H, Higashi K, Nieh TG (2004) Scripta Mater 50:395
18. Legros M, Elliott BR, Rittner MN, Weertman JR, Hemker KJ (2000) Philos Mag A 80:1017
19. Swygenhoven HV, Spaczer M, Caro A, Farkas D (1999) Phys Rev B 60:22
20. Hasnaoui A, Van Swygenhoven H, Derlet PM (2002) Acta Mater 50:3927
21. Wang Y, Chen M, Zhou F, Ma E (2002) Nature 419:912
22. Conrad H, Narayan J (2000) Scripta Mater 42:1025